Contrast-enhanced ultrasound (CEUS) of cystic and solid renal lesions: a review

Mittul Gulati,[1] Kevin G. King,[1] Inderbir S. Gill,[2] Vivian Pham,[1] Edward Grant,[1] Vinay A. Duddalwar[1]

[1]Department of Radiology, Keck USC School of Medicine, 1500 San Pablo Street, 2nd Floor Imaging, Los Angeles, CA 90033, USA
[2]Department of Urology, Keck USC School of Medicine, Los Angeles, CA, USA

Abstract

Incidentally detected renal lesions have traditionally undergone imaging characterization by contrast-enhanced computer tomography (CECT) or magnetic resonance imaging. Contrast-enhanced ultrasound (CEUS) of renal lesions is a relatively novel, but increasingly utilized, diagnostic modality. CEUS has advantages over CECT and MRI including unmatched temporal resolution due to continuous real-time imaging, lack of nephrotoxicity, and potential cost savings. CEUS has been most thoroughly evaluated in workup of complex cystic renal lesions, where it has been proposed as a replacement for CECT. Using CEUS to differentiate benign from malignant solid renal lesions has also been studied, but has proven difficult due to overlapping imaging features. Monitoring minimally invasive treatments of renal masses is an emerging application of CEUS. An additional promising area is quantitative analysis of renal masses using CEUS. This review discusses the scientific literature on renal CEUS, with an emphasis on imaging features differentiating various cystic and solid renal lesions.

Key words: Contrast-enhanced ultrasound—Renal mass—Renal cyst—Renal cell carcinoma

Renal lesions are detected in approximately 13–27% of adults undergoing cross-sectional abdominal imaging [1]. The majority of incidentally discovered renal lesions are simple cysts and can be confidently diagnosed on initial imaging exam. However, a significant minority do not meet criteria for simple cysts [2]. These include complex cystic and solid renal lesions.

Conventional ultrasound (US) can distinguish cystic from solid renal lesions and accurately diagnose simple and minimally complex cysts (Bosniak I and II equivalent). Multiphase contrast-enhanced computed tomography (CECT) and magnetic resonance imaging (MRI) have historically been the primary imaging modalities used to characterize and stage complex cystic and solid renal lesions [3].

Contrast-enhanced ultrasound (CEUS) evaluation of renal lesions is a relatively novel, but increasingly utilized, diagnostic modality. CEUS utilizes microbubble contrast agents to image blood flow and tissue perfusion. CEUS has been most thoroughly evaluated in workup of complex cystic renal lesions, where it has been proposed as a replacement for multiphase CT [4]. Using CEUS to differentiate benign from malignant solid renal lesions has been studied, but has proven difficult due to overlapping imaging features [5].

Monitoring minimally invasive treatments of renal masses, including cryoablation (CA) and radiofrequency ablation (RFA), in both intra-procedural and post-procedural settings, is an emerging application of CEUS. An additional promising area is quantitative analysis of renal masses using CEUS.

This review summarizes CEUS technique, followed by a comprehensive discussion of studies utilizing CEUS to evaluate renal masses.

Technique: Contrast-enhanced ultrasound of renal masses

CEUS relies on intravenous injection of encapsulated microbubbles of gas slightly smaller than a red blood cell, but much larger than particles used as CECT and MRI agents. The microbubbles therefore act as pure

Correspondence to: Mittul Gulati; *email:* mittul.gulati@med.usc.edu

intravascular contrast agents [6]. The microbubbles demonstrate non-linear oscillation between 3 and 5 MHz, which lies in the diagnostic range of US frequencies. After circulating for several minutes in the blood pool, the microbubbles dissolve. Internal gas is exhaled, and the coating, which may be protein, lipid, or polymer, is metabolized, primarily by liver [7].

Imaging advantages of CEUS include ability to detect microvasculature which can be overlooked by Color and Power Doppler US. While Doppler US can image blood vessels as small as 100 μm, CEUS can show vessels as small as 40 μm [8]. In addition, CEUS allows for high temporal resolution, with continuous dynamic imaging after injection as opposed to the intermittent static acquisitions possible with CECT and MR.

Most US machines used to interpret CEUS imaging have a split screen view, where contrast-enhanced images are presented on one screen and nonenhanced, gray scale images on the adjacent screen. This allows the examiner to observe enhancement pattern while remaining oriented to the anatomic area of interest. The most widely available CEUS technique relies on the principle of phase inversion. Two ultrasound pulses with 180 degree phase difference are sent consecutively. Echoes returning to the transducer are summated by the software, and as a result the linear echoes from body tissues null each other. In this manner, tissue signals are almost entirely canceled out, but contrast agent perfusing the tissues has a strong signal. Low mechanical index settings are used to allow detection of contrast agent and minimize microbubble destruction [9].

At our institution, patients referred for CEUS to evaluate a renal mass initially undergo unenhanced US exam using gray scale, Color, and Power Doppler. Size, morphology, echogenicity, and vascularity of the lesion are characterized. An intravenous line is inserted. For CEUS, hand bolus injection of 0.2 mL Definity® (Perflutren lipid microspheres, Lantheus Medical Imaging) or 0.5 mL Optison® (Perflutren Protein-Type A microspheres, GE Healthcare) is performed by the radiologist. Both agents have the option to rebolus multiple times. Complete real-time video clips of the CEUS examination are stored, with images acquired continuously for at least 2 min after contrast administration.

Renal CEUS exam contrast phase terminology is controversial, with numerous naming schemes used in literature, detailed later in this review. In practice, as well as for our figures, we utilize the following phase terms: corticomedullary (enhancing cortex with medullary pyramids not yet perfused, approximately 15–30 s post injection), nephrographic (homogenously enhancing renal parenchyma, approximately 30–70 s post injection), and delayed (>70 s post injection). Because these terms are typically used for multiphase CECT and MRI renal mass imaging, we find they translate easily for both radiologists and urologists.

The safety of Definity® and Optison® has been well documented, and both agents are FDA approved for echocardiography [10]. However, microbubble injection for non-cardiac applications, including renal mass evaluation, remains an off-label use in the United States.

A recently concluded multi-center Phase 3 study sought to address this issue. Trial BR1-128, sponsored by Bracco Diagnostics, enrolled 349 participants. The purpose of the study was to compare CEUS using BR1 (Sonovue®, Bracco) with unenhanced ultrasound in the evaluation of benign versus malignant focal liver lesions [11]. Truth standard was histology or imaging (CECT/MRI) data, and results are pending. In the meantime, Sonovue®, under the new trade name Lumason® (sulfur hexafluoride lipid-type A microspheres, Bracco Diagnostics), has recently been FDA approved for use in echocardiography [12]. Approval of Lumason® gives practitioners in the United States a third potential agent for off-label use in non-cardiac CEUS applications.

Safety advantages of CEUS include a low incidence of side effects and lack of nephrotoxicity. CEUS can be used in patients with iodine allergies and impaired renal function, which may be contraindications to contrast-enhanced CECT or MRI [13].

Limitations of CEUS in evaluation of renal lesions are largely those of the modality. Obese patients, poorly visualized kidneys, and shadowing from bowel gas or ribs can limit image acquisition.

Cystic renal lesions

Bosniak described the most widely accepted classification of renal cysts, initially published in 1986, and modified in 1993 [14, 15]. The classification system stratifies the malignant potential of cysts based on CECT features including wall, number and thickness of septations, presence of mural solid nodules, enhancement of septa and nodules, and calcifications. The 5 Bosniak categories (I, II, IIF, III, and IV) are ordered in increasing probability of malignancy. No further workup or intervention is required for category I and II lesions, whereas surgery is recommended for category III and IV lesions. Bosniak IIF lesions should undergo follow-up at 6 months, 1 year, and, due to slow growth of some low grade RCCs, should also undergo a 3–5 year follow-up [16, 17].

Utilizing CECT features and contrast enhancement, the Bosniak classification is highly accurate for predicting malignancy; heterogeneous cystic renal masses should be managed according to their most aggressive imaging features [18]. Application of Bosniak criteria to MR generally results in upgrading lesions to a higher category, due to increased MR detection of number, thickness, and enhancement of walls and septations [19].

Bosniak classification has been applied using CEUS, and a classification system proposed [20]. Several studies have shown CEUS to be more sensitive than CECT in

detecting septal vascularity. This finding has been attributed to CEUS better demonstrating tiny capillaries feeding fine septa [4, 21, 22]. CEUS has been proposed as the optimal modality to evaluate any complex cystic renal mass, with CECT then used to stage those lesions demonstrating malignant features on CEUS. In this algorithm, no enhancement on CEUS would necessitate no further workup [22].

Bosniak classification on CEUS is similar to CECT [23, 24]. A Bosniak I cyst has an anechoic lumen, well-defined back wall, no measurable wall thickness, and acoustic enhancement deep to the lesion. There is no potential for malignancy. Although there is no need to evaluate Bosniak I cysts with CEUS, if the exam is performed, no enhancement will be detected (Fig. 1).

A Bosniak II cyst may contain a few fine, thin septa, fine calcifications in the wall, or a short segment of thick wall calcifications. The walls and thin septa may show transient perceptible enhancement on CEUS, which may be better appreciated than on CECT. Lesions <3 cm with internal protein or hemorrhage (Bosniak II by CT) may fall into this category or appear as simple cysts (downgraded) on ultrasound. Bosniak II cysts again show no continuous enhancement, and no potential for malignancy, on CEUS.

Bosniak IIF cysts may have multiple fine, thin septa with continuous or prolonged enhancement on CEUS,

minimal thickening of wall or septa, and thick or nodular calcifications. Intrarenal homogenous lesions >3 cm with internal hemorrhage or protein also fit this category and are followed despite being well marginated and likely benign.

Bosniak III cysts have thickened, irregular, or smooth walls or septa with *measurable* rather than just perceptible enhancement. If quantitative analysis is not available, the qualitatively continuous or prolonged enhancement in thick or irregular walls/septa are classified as Bosniak 3. This category includes complicated cysts as well as multilocular cystic nephromas (now typically called mixed epithelial and stromal tumors) and some cystic RCCs. There are no enhancing soft tissue components.

Bosniak IV cysts have a high probability of malignancy and show clear-cut continuous or prolonged enhancement of soft tissue components independent of wall or septa (Fig. 2).

A summary of conventional US, CECT, and CEUS findings of cystic renal lesions, stratified by Bosniak classification, is provided in Table 1.

In practice, the greatest difficulty arises on all modalities in stratifying Bosniak II, IIF, and III lesions. As mentioned above, CEUS is more sensitive than CECT in detecting septal and wall vascularity. Observers may categorize enhancing septa or walls as thick or nodular on CEUS which are categorized as thin on CECT or
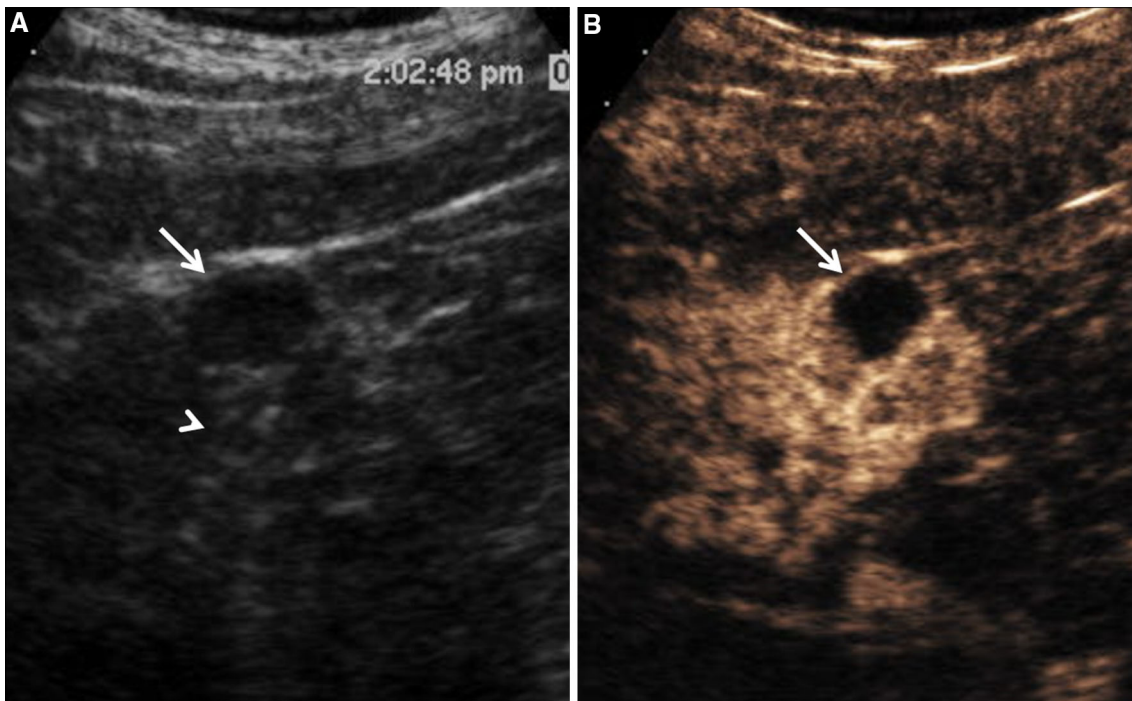

Fig. 1. An 83-year-old man with renal failure precluding CECT or MRI. Outside hospital ultrasound suggested a complicated cystic lesion at the lower pole of the left kidney. **A** Gray scale image demonstrates an anechoic lesion in the left renal cortex (*arrow*), with imperceptible anterior wall, thin echogenic posterior wall, and increased acoustic through transmission (*arrowhead*). Findings are consistent with simple (Bosniak 1 equivalent) cyst. **B** Nephrographic phase CEUS image shows no internal enhancement of the lesion (*arrow*), again diagnostic for simple cyst.
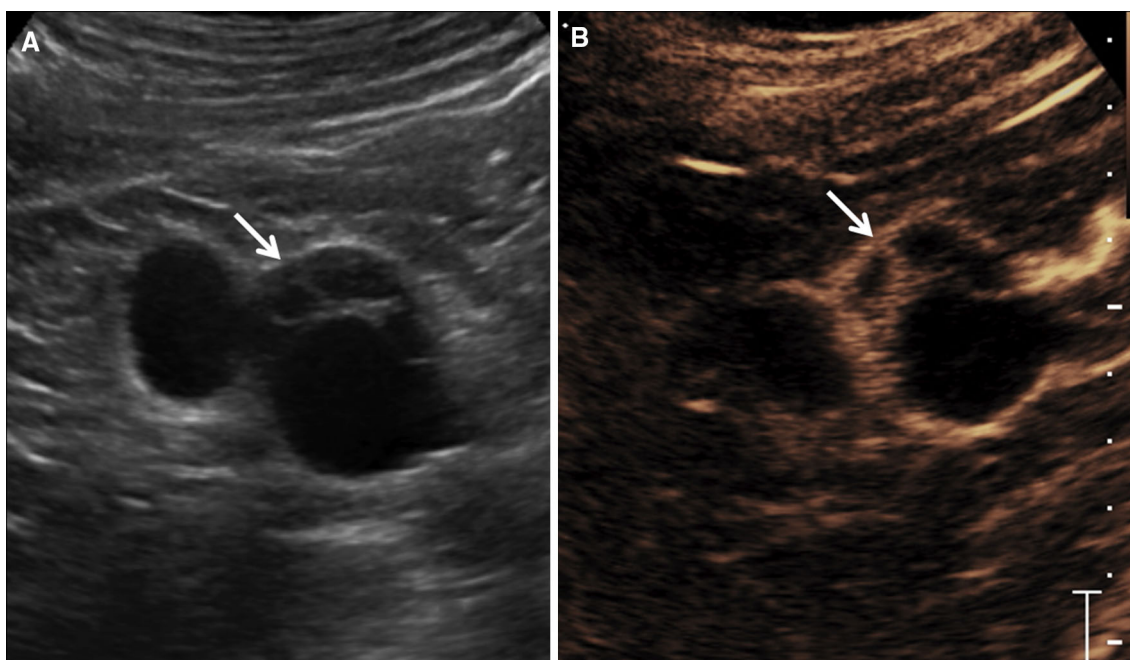
Fig. 2. A 79-year-old male with a complex right renal cystic lesion. **A** Gray scale image demonstrates a thick, complex septation (*arrow*) at the periphery of the larger of two adjacent cystic lesions. **B** Corticomedullary CEUS image demonstrates marked enhancement of the thick, complex septations (*arrow*). Following partial nephrectomy, pathology was multilocular cystic renal cell carcinoma.

Table 1. Overview of cystic renal lesions, their characteristic imaging features using conventional imaging modalities and CEUS features

Cystic lesion	Conventional US findings	CT findings	CEUS findings
Bosniak 1	Anechoic lumen, well-defined back wall, no measurable wall thickness, posterior acoustic enhancement	Fine thin wall, no septations, calcifications, or enhancement, Hounsfield units −10 to +20	No enhancement
Bosniak 2	Few fine, thin septa, fine wall, or septal calcifications	Same, as well as higher density lesions <3 cm size due to internal hemorrhage or protein. No enhancement	Thin septa may show transient perceptible enhancement
Bosniak 2F	Minimal regular or smooth thickening walls or septa; thick or nodular calcifications	Same, as well as high density lesions >3 cm size with internal hemorrhage or protein. No enhancement	Thin walls or septa may show continuous or prolonged enhancement
Bosniak 3	Measurably thickened or irregular walls or septa; or thick, nodular, and irregular calcifications	Same, as well as measurable enhancement >10 Hounsfield units	Thick or irregular walls or septa show continuous/prolonged enhancement
Bosniak 4	Soft tissue components independent of walls or septa; as well as class 3 features	Same, as well as measurable enhancement soft tissue components independent of walls or septa >10 Hounsfield units	Soft tissue components show continuous or prolonged enhancement

MR. The resultant upgrade to a Bosniak III cyst can result in a lesion classified as non-surgical by CT or MR become a surgical lesion by CEUS. In multiple studies, CEUS has resulted in upgrade of some lesions when compared with CECT [21, 25]. Although in these studies all lesions upgraded to category III or IV by CEUS were sent to the operating room, larger and long-term studies are needed to determine if the increased sensitivity of CEUS will result in an undesirable number of false-positive cystic RCC diagnoses.

A limitation of CEUS in evaluating cystic renal lesions includes posterior shadowing from wall or septal calcifications, which may limit visualization of intracystic enhancing nodules.

Solid renal neoplasms

Solid renal neoplasms can be of primary renal parenchymal or urothelial origin, or may be secondary neoplasms such as metastases or lymphoma. Most solid renal neoplasms are

Table 2. Overview of solid renal masses, characteristic imaging features with conventional imaging modalities, CEUS features, and references

Solid lesion	Conventional imaging findings	CEUS findings	References
Clear cell renal cell carcinoma (ccRCC)	US: variable. Small tumors often echogenic, can mimic AML. Larger tumors hypoechoic, exophytic, with central anechoic necrosis CT/MR: hyperenhances early (corticomedullary phase), hypoenhances later (nephrographic phase). Necrosis, hemorrhage, and calcification common	Shorter time to peak enhancement, as well as early hyperenhancement, relative to renal parenchyma Hypoenhancement ("washout") on delayed post-contrast imaging Perilesion rim-like enhancement ("pseudocapsule") Heterogeneous enhancement, which increases with lesion size	[30, 32, 35]
Papillary renal cell carcinoma	US: unilocular, hypoechoic CT: high attenuation non-contrast, hypovascular MR: hypovascular, T2 hypointense	Homogenous Hypoenhance to renal parenchyma throughout exam	[30, 32]
Angiomyolipoma (AML)	US: homogenously echogenic. However, lipid-poor AMLs can be isoechoic CT: measurable fat density (unless lipid-poor AML)	Variable features observed Homogenous, hypoenhance to renal parenchyma Persistent (greater delayed) enhancement compared with ccRCC	[27–29, 32–34]
Oncocytoma	US: central scar may be hypoechoic. Color Doppler may show central radiating vessels CT: well defined, homogenous, noninvasive. Central fibrous scar may be seen	Hyperenhance to renal parenchyma early, persistent (greater delayed) enhancement compared with ccRCC Enhance from periphery to center	[31, 38–40]
Pseudotumor	US: size <3 cm, similar echogenicity to renal parenchyma, clear demarcation from renal sinus, regular branch-like blood flow CT/MR: identical enhancement pattern to renal cortex	Identical enhancement to surrounding renal cortex throughout exam	[37, 47, 48]
Metastases	CT: Small, low density, usually bilateral, most hypovascular after contrast (melanoma may be hypervascular)	Typically hypovascular to renal cortex throughout exam	[25, 27]
Lymphoma	US: hypoechoic, may mimic renal cyst CT: multiple bilateral masses (60%), direct extension from retroperitoneal nodes (25%), solitary mass 1 kidney (15%), almost always in seen in background widespread systemic lymphoma. When renal masses, usually minimal enhancement	Limited data May be hypovascular to renal cortex throughout exam	Unpublished observation

incidentally detected. A summary of conventional imaging (US, CECT, and MRI) findings, as well as CEUS findings, of solid renal lesions is provided in Table 2.

The most common solid renal neoplasm is RCC, with an increasing incidence in the United States, where approximately 63,400 new cases are currently diagnosed each year. RCC is the 7th leading cancer type in men in the U.S [26]. The gender ratio of RCC in the U.S. is approximately 2:1 for males:females. Between 1971 and 2010, there was a 5-fold increase in incidence of, and a two-fold increase in death from, RCC in the U.S. [27].

Renal cell carcinoma and angiomyolipoma

A main goal of imaging renal masses is to differentiate malignant lesions, most often RCC, from benign entities such as angiomyolipoma (AML) and oncocytoma [28]. RCC is characterized by numerous thin-walled blood vessels with rich blood flow, and common findings include intra-tumoral necrosis, hemorrhage, and calcification [29]. Historically, CECT or MRI has been used to characterize solid renal masses [30]. Clear cell RCC (ccRCC), the most common variant, typically hyperenhances in early (corticomedullary) and hypoenhances relative to normal renal parenchyma on nephrographic phase CECT exams. Typical AMLs contain macroscopic fat and have negative Hounsfield unit measurements on non-contrast CT. CECT and MRI are limited in diagnosis of lipid-poor AMLs and oncocytomas.

US has low ability to show microvascularity in RCC, and echogenicity has not proven specific in differentiating RCC from benign solid renal lesions. For example, Forman showed that 77% of small RCCs showed variable echogenicity, and 32% were hyperechoic enough to mimic renal AMLs [31]. Conversely, although AMLs are typically homogenously echogenic, lipid-poor AMLs may appear isoechoic on US [32]. Just as US echogenicity cannot reliably differentiate solid renal masses, conventional color Doppler US may have low ability to detect intra-tumoral vascularity in RCCs, with 41% sensitivity in one series [33].

Numerous studies have utilized CEUS, in combination with conventional ultrasound, to characterize solid renal masses. Results have been mixed leading some

groups to conclude that CEUS is of limited utility in characterizing solid renal masses due to overlapping features of benign and malignant lesions [34]. However, other studies have described specific CEUS features associated with RCC and other renal neoplasms. The studies are not all directly comparable, in part due to differences in terminology; some groups describe "arterial and delayed" phases as <30 and 30–90 s after microbubble injection [35], while other groups describe cortical (approximately 8–35 s after injection), corticomedullary (36–120 s), and delayed (>120 s) phases [33]. In practice, as well as for the figures in this review, we utilize the terms corticomedullary, nephrographic, and delayed phase CEUS imaging, analogous to multiphase CECT or MRI. Our rationale for using these terms is detailed in the techniques section.

Several early studies utilized SHU508 (Levovist®), a first-generation contrast agent with reticuloendothelial system uptake. In contrast, more recent studies have utilized purely intravascular contrast agents such as BR1 (Sonovue®).

One early study utilizing SHU508, performed by Ascenti et al. in 2001, examined 41 hyperechoic renal lesions in 32 patients with power Doppler and CEUS, in an attempt to stratify AML from RCC (final pathology 26 AML, 11 RCC, 3 pseudotumor, 1 metastasis). Most AMLs in the study showed no detectable vessels, a spotty or linear intra-tumoral vascular pattern not extending to the periphery of the lesion, or a penetrating pattern with vessels arising outside the lesion and coursing toward its center. All RCCs showed peripheral and central enhancement. However, the RCC perfusion patterns were not specific; several AMLs also showed peripheral or central enhancement. Although CEUS and power Doppler increased diagnostic accuracy to 78% vs. 32% for grayscale ultrasound alone, the authors concluded that adding CEUS did not increase the diagnostic accuracy over power Doppler [30].

Quiaia et al. investigated 23 lesions (15 RCC, 7 AML, 1 metanephric adenoma) by CEUS, also using SHU508. They found that solid RCCs revealed much higher peak contrast enhancement than typical AMLs; however, both an atypical AML and a metanephric adenoma in their cohort showed similarly intense arterial phase enhancement [36].

Fan et al. used CEUS to examine 72 lesions <5 cm in size with BR1 (44 RCC, 24 AML, 2 hypertrophied columns of Bertin, 1 oncocytoma, 1 abscess). The enhancement pattern of all lesions was classified as heterogeneous or homogenous, and lesions were characterized in arterial (<30 s after injection) and "late" (30–90 s after injection) phases. Heterogeneous arterial enhancement and "late" hyperenhancement predicted ccRCCs, with a sensitivity of 77.3% and specificity of 96.4%. All papillary and chromophobe RCCs, as well as 12.8% of ccRCCs, were hypoenhancing in arterial and late phases. Renal AMLs were more often homogenous (75%) and hypoenhanced (83.3%) in both arterial and late phases. The authors concluded that CEUS was poor for differentiating hypovascular RCCs from AMLs [35].

Xu et al. retrospectively evaluated 84 RCCs examined with BR1. They divided enhancement phases into cortical (8–35 s), corticomedullary (36–120 s), and delayed (>120 s), with timing referenced to the CEUS injection. They found most RCCs showed hyper- or isoenhancement to background renal parenchyma during cortical phase, hypoenhancement ("washout") relative to renal parenchyma in corticomedullary phase, heterogeneity, and perilesional rim-like enhancement. The authors also found that RCCs >3 cm in diameter were more heterogeneous than smaller tumors, and that papillary RCCs showed hypoenhancement throughout the cortical phase and were more homogenous than ccRCCs [33]. The lack of benign lesions in the study precluded analysis of specificity of features described for malignancy. However, another study by the same group, which included 93 RCCs and 33 AMLs, found that homogenous enhancement and delayed enhancement were characteristic of AMLs [37].

Similar conclusions regarding RCCs were reached in a retrospective study of 92 ccRCCs evaluated by BR1 by Jiang et al. Their study retrospectively correlated tumor size with CEUS findings and concluded that homogenous enhancement was seen in 72% of tumors <3 cm in size, but only in 9% of tumors >3 cm in size. They also noted a "pseudocapsule" (rim of perilesion enhancement) most frequently in tumors 2.1–5 cm in size (66%) and less often in tumors <2 cm (23%) and >5 cm (24%) [38]. Again, these features were largely descriptive, and analysis of diagnostic specificity was precluded by the nature of the study.

Given the contradictory conclusions reached by individual studies, a recent meta-analysis addressed the accuracy of CEUS for differentiating RCC from benign renal lesions. The authors identified 11 studies including both benign and malignant lesions, with a total of 567 RCC and 313 benign renal tumors in the database. All studies utilized BR1 as the CEUS agent. Pooled sensitivity, specificity, and diagnostic odds ratio were 88, 80, and 46.97, respectively. The authors concluded that CEUS may have a high diagnostic accuracy and be a valuable tool for RCC diagnosis [39].

Although consistent features are not described across all studies, a summary of features can be derived from review of the literature [33, 35, 38]. CcRCCs typically show early hyperenhancement relative to renal parenchyma, hypoenhancement ("washout") on delayed phase, and perilesion enhancement. Tumor heterogeneity is a common CEUS feature of ccRCCs and is more prevalent with increased lesion size (Fig. 3). Papillary and chromophobe RCCs as well as AMLs are typically hypoenhancing and homogenous on CEUS (Fig. 4).
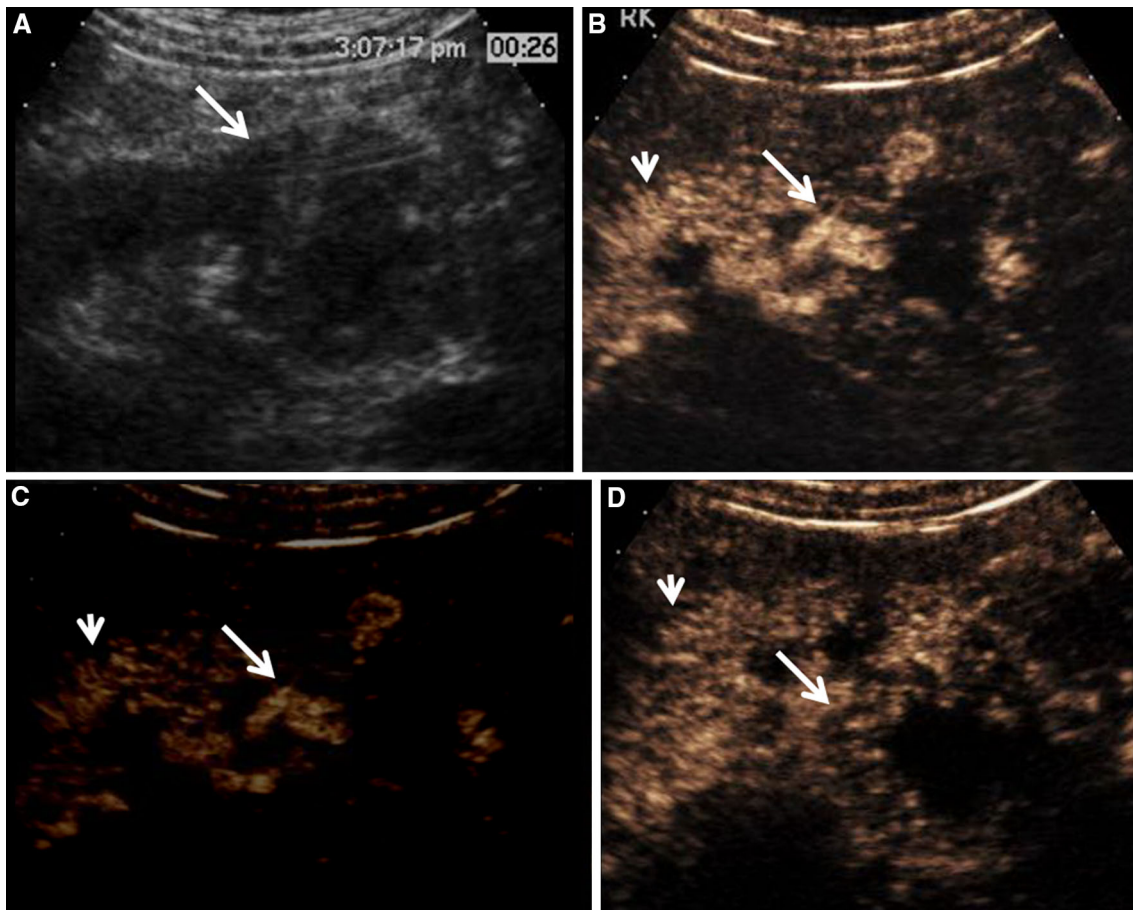
Fig. 3. A 62-year-old man with renal failure and incidental right renal mass. **A** Gray scale image demonstrates a heterogeneous, partially exophytic mass (*arrow*) at the lower pole of the right kidney. **B** Corticomedullary CEUS image demonstrates avid enhancement (example, *arrow*) at the periphery of the mass, with no enhancement of the necrotic center. Normal renal cortex (*arrowhead*) enhances less avidly than the periphery of the mass. **C** Narrow window settings at the same early perfusion CEUS time point as **B** better demonstrates that the peripheral enhancing components of the mass (*arrow*) enhance more intensely than normal renal cortex (*arrowhead*). **D** Delayed perfusion CEUS image demonstrates washout of the mass (*arrow*) compared to normal adjacent renal cortex (*arrowhead*). Following partial nephrectomy, pathology was clear cell renal cell carcinoma.

Oncocytoma

Oncocytomas are considered benign lesions and can be difficult to differentiate pathologically from chromophobe RCC of low malignant potential [40]. Imaging diagnosis is also difficult. Choudhary et al. described CECT findings in 21 patients with 28 histologically confirmed oncocytomas. Enhancement was isodense in 64% and hypodense in 36% relative to renal cortex. 18% of lesions showed a fibrous central scar, a feature often described in oncocytoma. The authors concluded that CECT failed to demonstrate typical imaging features in oncocytoma [41].

There have been relatively few reports of oncocytoma features on CEUS. Strobel et al. found a central scar on none of three oncocytomas, and found 2 of 3 were hypervascular and 1 of 3 hypovascular in arterial phase. On delayed imaging, all 3 were hypovascular relative to renal paren-

chyma [34]. Tamai et al. found that 1 of 2 oncocytomas showed a spoke wheel configuration of vessels on CEUS, allowing correct preoperative diagnosis of oncocytoma [42].

Wu et al. examined 5 oncocytomas by CEUS and designated contrast phases as cortical, corticomedullary, and delayed, with identical time points as the study by Xu et al. above [33]. Wu found that all 5 oncocytomas filled from periphery to center during the cortical phase, hyperenhanced relative to normal renal parenchyma, and that hyperenhancement persisted through corticomedullary phase, as opposed to most RCCs which hypoenhanced by corticomedullary phase. Wu saw areas of irregular non-enhancement centrally on 3 of 5 oncocytomas and suggested that these correlated with fibrous scars seen at gross pathology. They did not observe a spoke wheel enhancement pattern on any cases. The authors concluded that prospectively differentiating
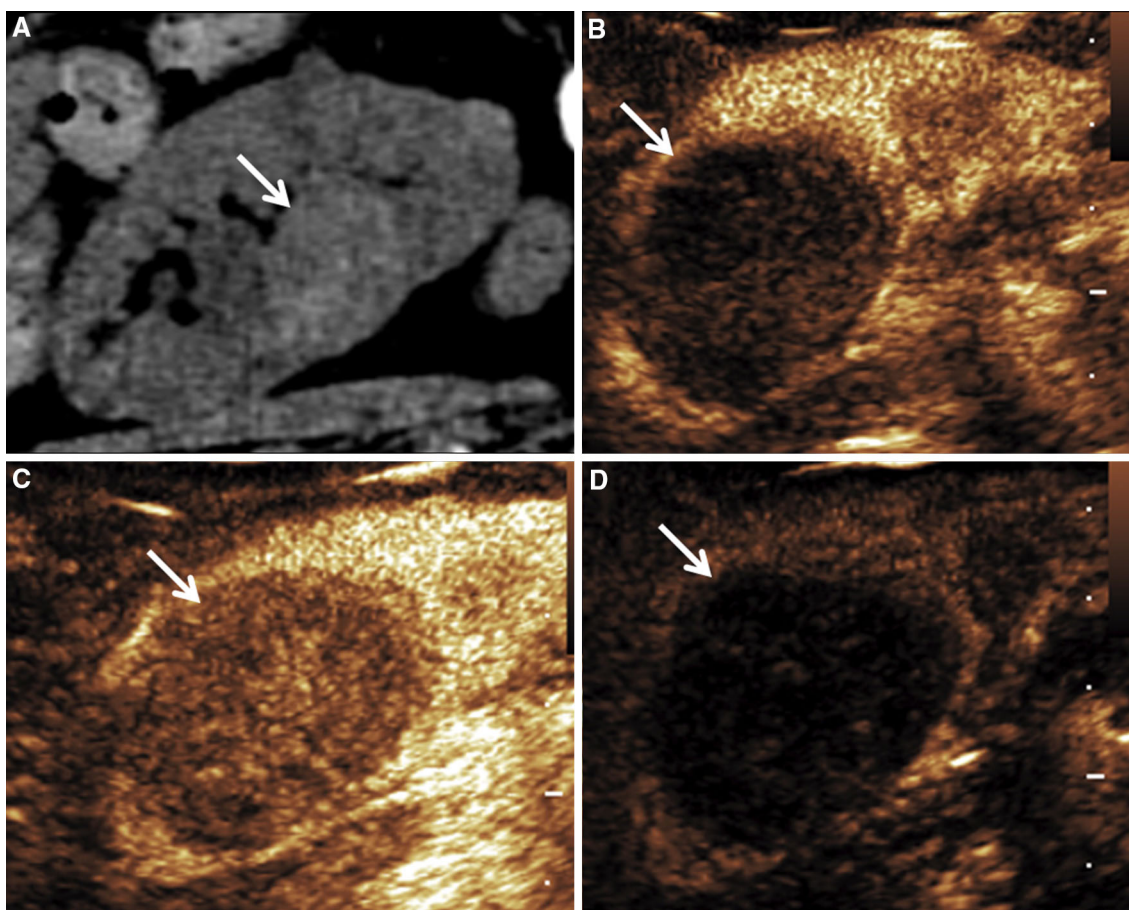
Fig. 4. A 76-year-old woman. **A** Non-contrast CT demonstrates hyperdense left renal mass (*arrow*). There are additional smaller left renal lesions. **B** On corticomedullary CEUS image, mass (*arrow*) is markedly hypovascular to renal parenchyma. **C** On nephrographic CEUS image, mass shows mild homogenous internal enhancement, but is again hypovascular to renal parenchyma. **D** On delayed CEUS image, mass is persistently hypovascular to renal parenchyma. Following partial nephrectomy, pathology was type I papillary RCC.

oncocytoma from RCC by imaging is difficult, with poor predictive value [43].

In our experience, oncocytomas typically hyperenhance to renal parenchyma early and can show persistent enhancement through delayed phase on CEUS (Fig. 5).

Pseudotumors

The term renal pseudotumor most commonly refers to mass-like anatomic variants including persistent fetal lobulation, hypertrophied column of Bertin, and dromedary hump. Conventional US features of pseudotumors include location between overlapping portions of two renal sinus systems, clear demarcation from the renal sinus, size < 3 cm, similar echogenicity to renal parenchyma, lesion being bordered by a junctional parenchymal line, and demonstrated regular, branch-like blood flow in the lesion [44].

In practice, it can be difficult to distinguish pseudotumors from pathologic lesions on US. For example,

infiltrative lesions which do not deform the renal surface, such as metastases and lymphoma, can mimic a pseudotumor [45]. Although color and power Doppler may be useful to evaluate the vascular pattern of a suspected pseudotumor, both techniques have poor sensitivity in patients who are obese or have difficulty in breath holding [46, 47]. CECT or MRI are often used to characterize a possible renal pseudotumor, due to their added value in vascular characterization [48, 49].

Mazziotti et al. performed CEUS on 24 patients with possible pseudotumors on US. Their CEUS diagnoses included hypertrophied column of Bertin (14), persistent fetal lobulation (5), RCC (2), and metastases (3). CEUS was concordant with CECT or MRI in all cases (specificity, PPV, and NPV 100%). Cases of RCC and metastases had final diagnoses obtained by renal biopsy or surgical resection. The main CEUS criterion for diagnosis of renal pseudotumor was enhancement of the lesion identical to renal cortex in all post-contrast phases of the exam. The authors concluded that CEUS can
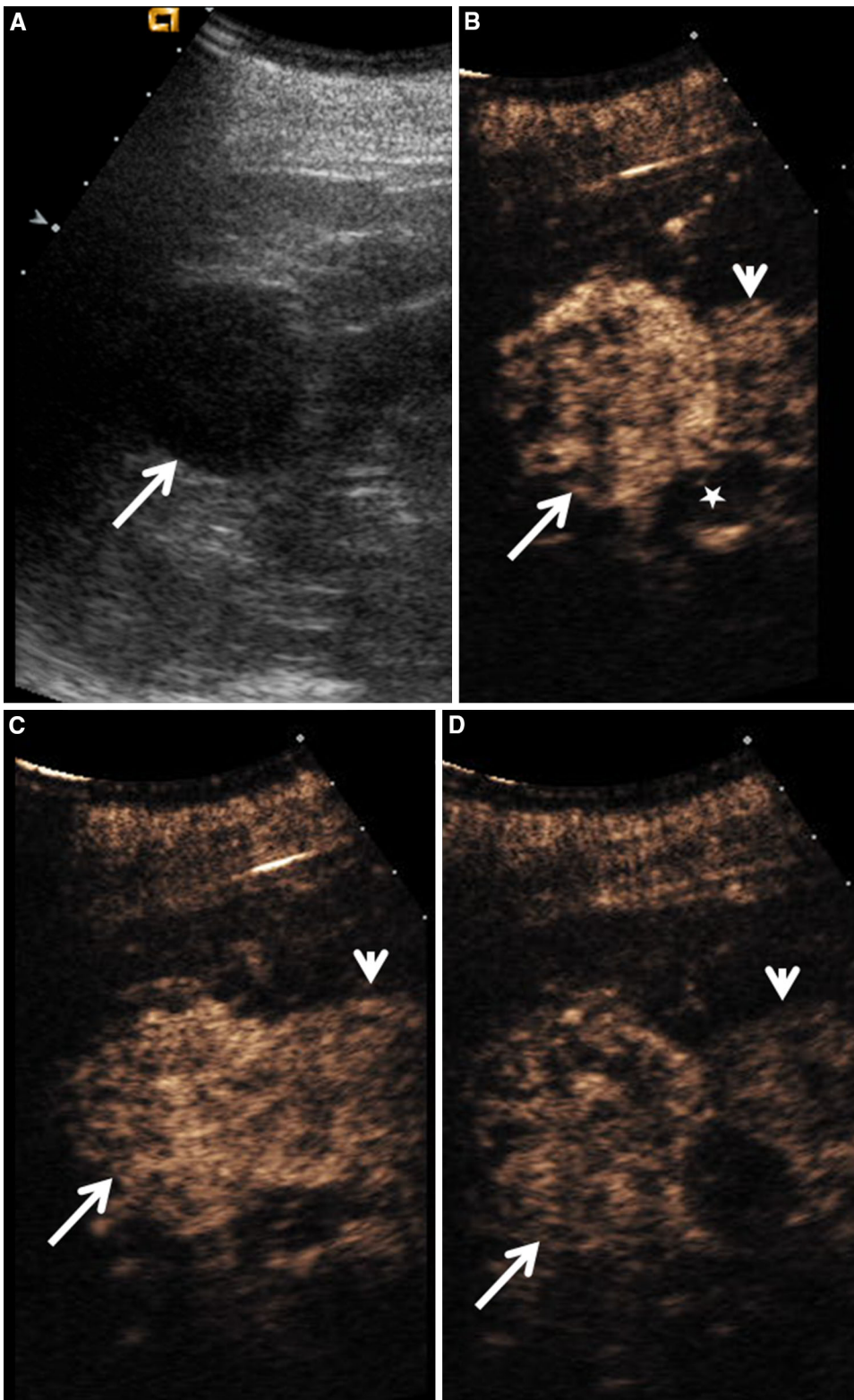
Fig. 5. An 86-year-old male patient with a right renal mass. A Echogenic, exophytic, well-circumscribed right renal mass (*arrow*) on gray scale ultrasound. B Corticomedullary CEUS image shows early avid enhancement of the mass (*arrows*), relative to normal renal parenchyma (*arrowhead*). There is a small simple cyst posterior to the mass (*star*). C Nephrographic CEUS image demonstrates persistent avid enhancement of the mass (*arrow*) compared to normal renal parenchyma (*arrowhead*). D Delayed CEUS image (100 s) shows some de-enhancement of the lesion (*arrow*), which still enhances to a greater degree than normal renal parenchyma (*arrowhead*). Following partial nephrectomy, pathology was oncocytoma.

reduce the need for CECT or MRI for diagnosis of renal pseudotumors [50].

Ascenti et al. also had 4 pseudotumors (1 persistent fetal lobulation, 2 column of Bertin, 1 RCC) with equivocal Doppler US findings, which they examined by CEUS. Pseudotumors were diagnosed by a characteristic vascular pattern in which they showed identical vascularity to surrounding renal parenchyma, without pene-
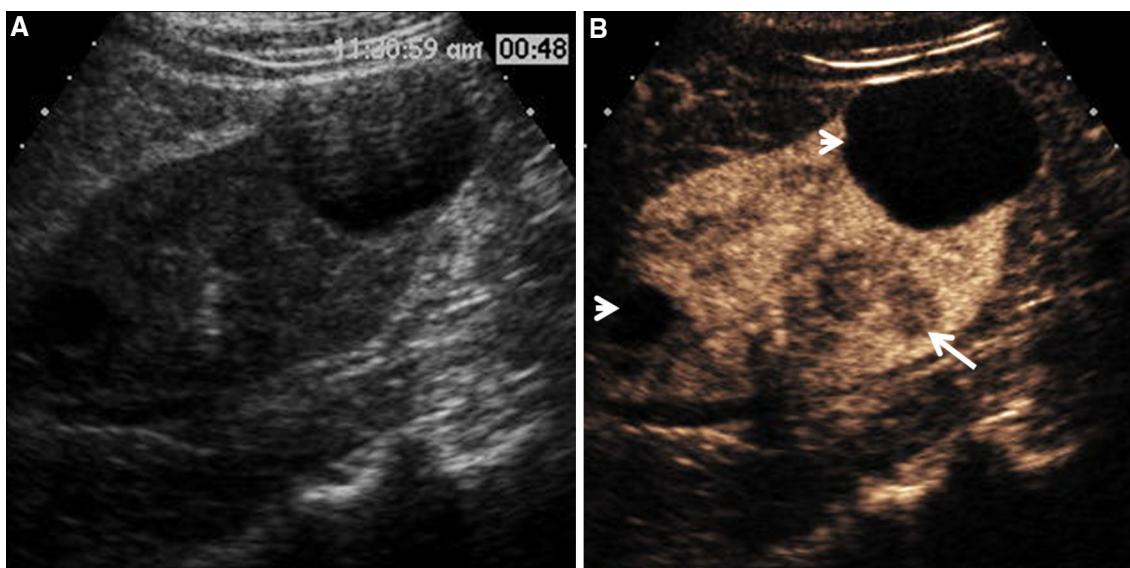
Fig. 6. A 71-year-old male with widespread metastatic melanoma. Hypovascular right renal mass on CT. **A** Gray scale images do not clearly demonstrate a focal lesion. **B** Nephrographic phase CEUS image demonstrates a focal hypovascular lesion (*arrow*). There are also Bosniak I simple cysts (*arrowheads*). Pathology was consistent with metastatic melanoma.

trating or peripheral vessels. The authors concluded that CEUS added diagnostic value to color and power Doppler US (37).

In a recent large study of CEUS in 1018 lesions, Barr found that CEUS confidently identified pseudotumors including 63 congenital fusion anomalies and 6 parenchymal scars [51].

In addition to anatomic variants, the term renal pseudotumor can also refer to mass-like infectious processes, such as focal pyelonephritis or renal abscess [52]. A study by Fontanilla et al. used CEUS to evaluate 48 patients with complicated acute pyelonephritis (APN), defined as APN not responding to 72 h of antibiotics. They divided CEUS exams into cortical (15–30 s), early parenchymal (30 s to 1 min), and late parenchymal (1–4 min) phases, based on time after injection. The authors described CEUS features which differentiated focal pyelonephritis from renal abscess. On CEUS, renal abscess demonstrated complete absence of enhancement throughout all phases. Focal pyelonephritis, on the other hand, manifested as a wedge-shaped or round area of hypoenhancement, best appreciated on late parenchymal phase. There was excellent correlation with clinical course, follow-up CEUS exams, and available CECTs. The authors noted that in their institution, CEUS had replaced CECT as the first-line imaging exam for complicated APN [53].

Available data suggest CEUS may be of value in diagnosing anatomic and infectious pseudotumors, with similar accuracy to CECT or MRI.

Metastases and lymphoma

Renal metastases are typically detected when a nonrenal primary progresses, and median survival is very short [54]. Solitary renal metastases have been reported in the setting of numerous primary malignancies [55].

Primary renal lymphomas are very rare; secondary renal involvement by lymphoma in the background of systemic lymphoma is 30 times more common.

Typical imaging features of both renal metastases and lymphoma include size <3 cm, lack of spherical shape, "infiltrative" growth, multiplicity, bilaterality, and lack of encapsulation or calcifications [56].

Few studies have reported CEUS findings in metastases. Lassau et al., in a study monitoring advanced RCC patients undergoing antiangiogenic therapy with Soafenib, had 2 patients in their cohort with contralateral renal metastases. However, limited description was provided of the CEUS enhancement pattern of these metastases prior to therapy. Available data suggest that the most renal metastases are hypovascular on all phases [28, 30], which correlates with our experience (Fig. 6).

There is a paucity of published data regarding CEUS characteristics of renal lymphoma. However, we observed a case which arose in a renal allograft where the lymphoma was hypovascular throughout renal perfusion (Fig. 7).

CEUS for monitoring of interventions

Emerging applications of CEUS include both monitoring after and during interventions. Local therapies, including
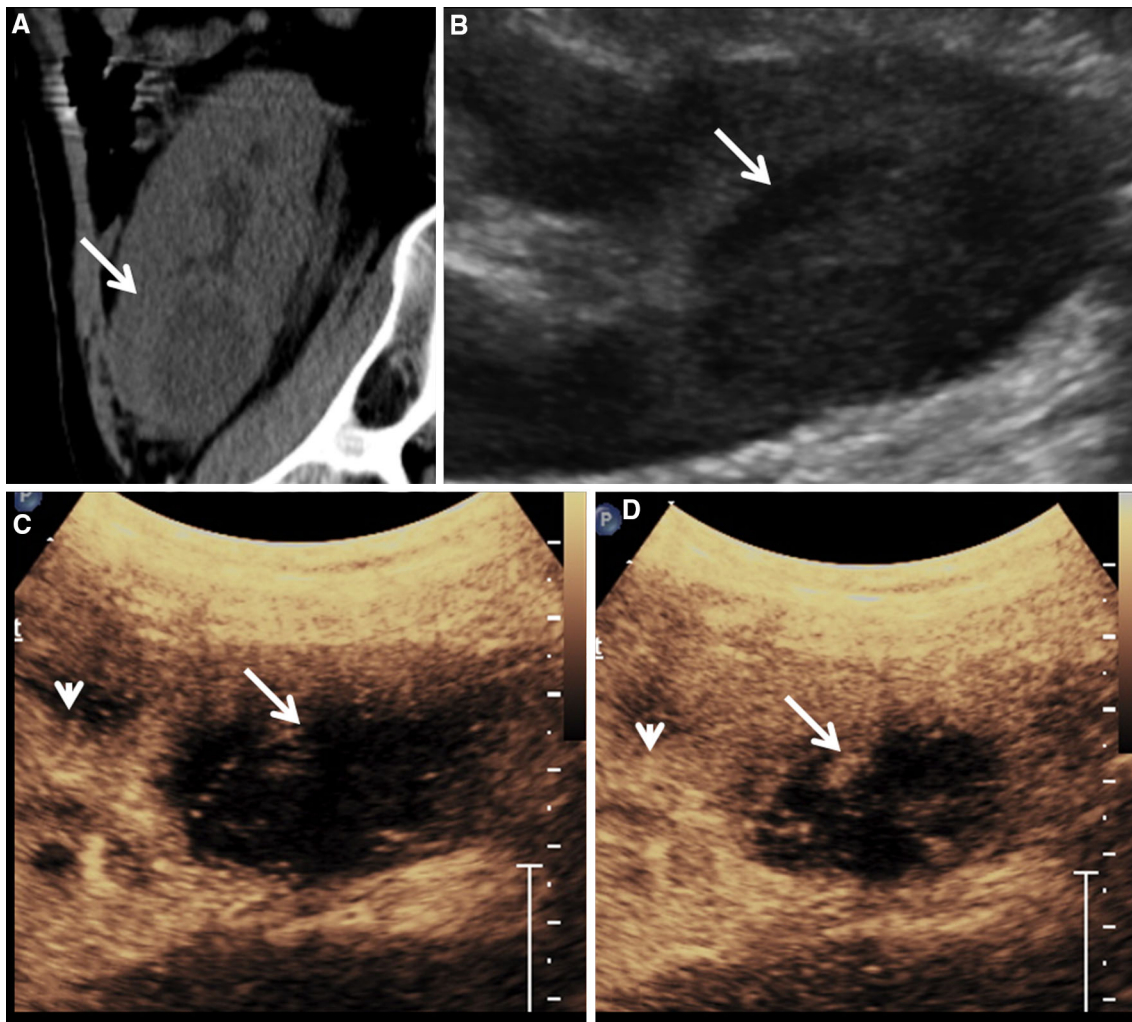
Fig. 7. A 77-year-old man with remote right lower quadrant renal transplant. A Non-contrast CT shows round, centrally hypodense mass at the lower pole of the transplant kidney (*arrow*). B Gray scale image showed hypoechoic mass (*arrow*) corresponding to finding on CT. C Corticomedullary CEUS image demonstrates hypovascular mass (*arrow*) rela- tive to renal parenchyma (*arrowhead*). D Nephrographic phase image demonstrates minimal peripheral enhancement in the mass (*arrow*), which remained persistently hypovas- cular to normal renal cortex (*arrowhead*) throughout the exam. Pathology revealed lymphoma (post transplant lymphoprolif- erative disorder).

RFA and CA, can be used with curative intent to treat small RCCs.

CEUS after CA was evaluated in a pilot study by Wink examining 7 patients. All patients had a CEUS exam, which was compared with CT. Wink used a CEUS scoring system in which 0 = no enhancement, 1 = rim enhancement, 2 = diffuse enhancement, 3 = localized enhancement, 4 = no defect in enhancement. In the majority of patients, no enhancement (a score of 0) was seen at either CEUS or CT. The one tumor which did show enhancement of an ablated RCC demonstrated that finding on both CEUS and CECT [57].

A larger study examining CEUS in evaluation of cryolesions was published by Barwari et al. They com- pared CEUS to CECT or MRI, at time points before, 3 months after, and 12 months after CA. Barwari used the same scoring system as Wink, and found good cor- relation between CEUS and CECT/MRI. For example, at 12 months after CA, enhancement score corresponded on both modalities in 19 of 21 patients, with 2 showing enhancement on CEUS without enhancement on CECT/ MRI (specificity 90%, NPV 100%). Correlation was lower at initial (3 months) post-treatment scan. The authors suggested that while CECT/MRI should be used to demonstrate successful ablation at first follow-up, CEUS could be used to diminish cost burden and nephrotoxicity for subsequent follow-up exams [58].

Real-time intraprocedure monitoring during RFA was evaluated by Chen et al. The authors conducted a randomized surgical trial. 96 patients undergoing lapa- roscopic RFA of renal lesions were randomly assigned either to a control group, or to a group in which intra-
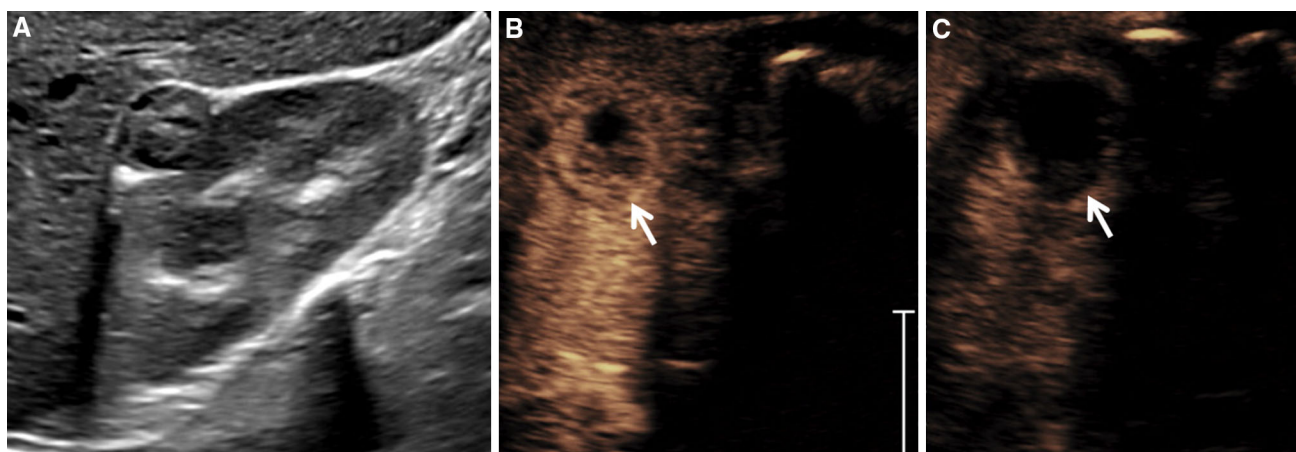
Fig. 8. A 29-year-old female with a right renal mass. **A** Gray scale image reveals a well-circumscribed, solid, heterogeneous, exophytic mass arising from the right kidney. **B** Corticomedullary CEUS image demonstrates peripheral enhancement of the mass (*arrow*), with a non-enhancing center. **C** Delayed perfusion CEUS image demonstrates washout of the mass (*arrow*) compared to normal adjacent renal cortex. Following partial nephrectomy, pathology was clear cell renal cell carcinoma.

operative CEUS was performed just before and after RFA. CEUS immediately after RFA showed no enhancement of the treated lesion in 44/48 patients. The 4/48 CEUS patients with tumors showing residual enhancement underwent additional ablation and repeat CEUS at the same RFA session. In a mean 16-month follow-up period, there were three incomplete ablations and two local recurrences in the control group. There were no incomplete ablations or local recurrences in the CEUS group. Local tumor control rate was 87.5% in the control group, versus 100% in the CEUS group. Although the study was not powered to reach statistical significance, there was a nonsignificant trend in favor of CEUS. Whereas conventional monitoring during RFA consisted of probe tip temperature monitoring and needle position confirmation by ultrasound only, CEUS provided the operator with a real-time perfusion deficit map [59].

Quantitative imaging

Quantitative analysis of RCC and other renal masses is an emerging application of CEUS. Such analysis relies on software which generates time–intensity curves (TIC), which plot echo intensity against time. TIC of both lesion (a manually determined region of interest, or ROI, selected by the radiologist) and normal renal parenchyma are performed for comparison.

Dong et al. reviewed CEUS exams on 42 patients with pathologically proven ccRCC. They found that 9 smaller tumors showed homogenous enhancement, while 33 larger tumors showed heterogeneous enhancement. They found that there was NOT a characteristic perfusion pattern for RCCs in their study. However, they did divide their quantitative analysis into 4 patterns of RCC

perfusion. Type 1 was rapid enhancement, with rapid washout relative to normal renal parenchyma (11/42), type II was rapid enhancement with slow washout relative to renal parenchyma (17/42), type III was tumors which both enhanced and "washed out" simultaneously to normal renal parenchyma (7/42), and type IV was slow enhancement with slower washout than renal parenchyma (7/42). Although no characteristic perfusion pattern could be ascribed to all ccRCCs, the authors did "quantify" that in their subjects time to peak (TTP) of tumors was shorter than that of normal renal parenchyma, confirming a frequently observed feature [60].

Cai et al. recently published a quantitative analysis of 73 renal masses, which included 46 ccRCC (ccRCC), 4 papillary and 2 chromophobe RCC, 16 AMLs, 2 renal abscesses, 2 columns of Bertin, and 1 oncocytoma. They found that RCCs measured larger on CEUS than on conventional US exam. The authors discussed their observations that most ccRCCs enhance more quickly, and hyperenhance at TTP, compared with normal renal parenchyma [28, 61]. This has been our experience as well with TICs of ccRCC (Figs. 8, 9). However, quantifying enhancement in the washout phase of RCC is controversial, and Cai explored this area with quantitative analysis. They found 2 quantitative criteria which, in combination, were 44% sensitive and 99% specific for differentiating benign and malignant renal lesions. The first criterion analyzed the portion of the lesion with peak enhancement; this area was found to wash out more rapidly than normal renal parenchyma, with a threshold time of >4.74 s established to differentiate benign and malignant lesions. The second criterion evaluated the lesion as a whole at 60 s post-injection; this was termed the "washout phase," a time point not to be confused with qualitatively observed or quantitatively analyzed
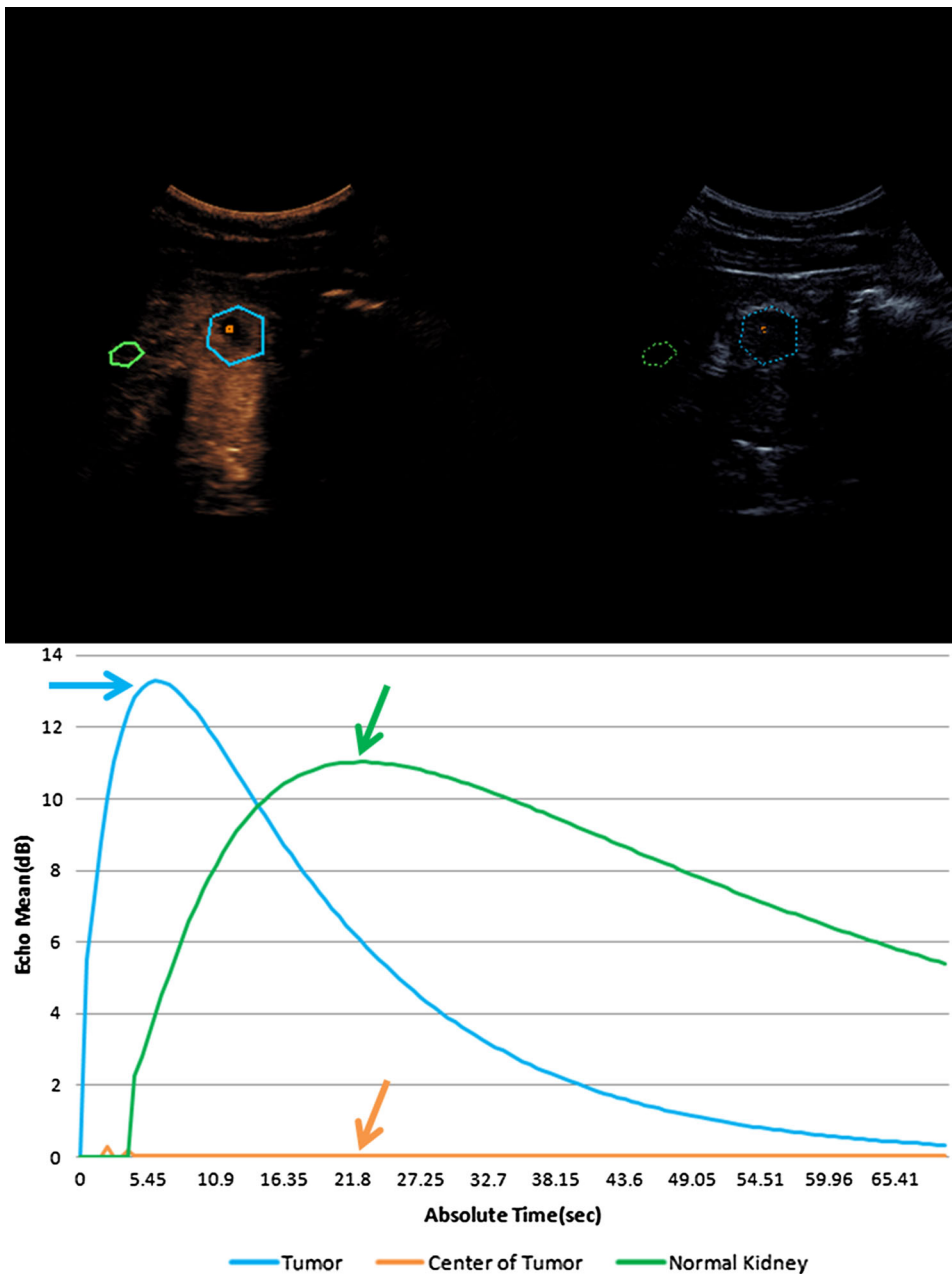
Fig. 9. Contrast kinetics of a pathologically proven ccRCC, the same case as Fig. 8. The horizontal axis on the table is time in seconds, plotted against echo mean in decibel (dB) on the vertical axis. Echo mean quantifies peak enhancement of a given region of interest (ROI). ROIs are plotted throughout the CEUS exam, and curves of best fit drawn to connect the points. The two small upper inset images are example ROIs from early (*left*) and later (*right*) in the CEUS exam. The blue ROI is located within the tumor, and represented by the blue curve, which shows quick time to peak and high peak intensity (*blue arrow*). Normal renal cortex is the *green* ROI, showing a slower time to peak and lower peak intensity (*green arrow*) relative to tumor. The center of the tumor is necrotic (*orange* ROI), with no appreciable enhancement (*orange arrow*) throughout the exam.

washout of contrast. The authors found that the lesion still hyperenhanced overall at this 60 s time (the "washout phase") relative to background renal parenchyma, with a cutoff of the whole lesion enhancing $>8.52\%$ more than background renal cortex at 60 s was specific for malignancy [62]. Of note, we have not replicated this final finding; in our subjects, we have seen delayed phase hypoenhancement ("washout") of ccRCCs relative to normal renal parenchyma, with both qualitative (Figs. 3, 8) and quantitative (Fig. 9) analysis.

Although quantitative analysis is an emerging application, it holds great potential for stratifying renal masses into benign and malignant lesions for purposes of clinical management.

Conclusion

Reaching conclusions from CEUS studies evaluating renal masses is limited by use of varying contrast agents, lack of standardized terminology regarding phase of contrast, and heterogeneity of scanning technique. However, these are expected challenges for any emerging imaging application. Review of studies does, nevertheless, allow a number of conclusions.

For cystic renal lesions needing further evaluation, CEUS is an excellent imaging modality, equivalent to multiphase CECT and MR. A major caveat is that applying Bosniak criteria, CEUS will upgrade a percentage of lesions compared with CECT, due to the

increased sensitivity of CEUS for septal enhancement. For solid renal lesions, CEUS is excellent for diagnosis of pseudotumors, again comparable to CECT and MR.

CEUS results are mixed in differentiating RCC from benign lesions. Most ccRCCs hyperenhance, show peak enhancement earlier than renal parenchyma, and demonstrate increasing heterogeneity with larger lesion size. There can be overlap of RCC imaging features with oncocytomas. Similarly, there can be overlap between hypovascular malignant renal lesions, such as papillary RCCs and lipid-poor AMLs.

Emerging areas of study include CEUS for monitoring interventions, including CA and RFA, of renal masses. Finally, quantitative imaging, via analysis of TICs taking advantage of the high temporal resolution of CEUS, holds great promise for stratifying benign and malignant lesions.

References

1. Gill IS, Aron M, Gervais DA, Jewett MA (2010) Clinical practice. Small renal mass. N Engl J Med 362(7):624–634
2. O'Connor SD, Silverman SG, Ip IK, Maehara CK, Khorasani R (2013) Simple cyst-appearing renal masses at unenhanced CT: can they be presumed to be benign? Radiology 269(3):793–800
3. Kang SK, Chandarana H (2012) Contemporary imaging of the renal mass. Urol Clin North Am 39(2):161–170
4. Ascenti G, Mazziotti S, Zimbaro G, et al. (2007) Complex cystic renal masses: characterization with contrast-enhanced US. Radiology 243(1):158–165
5. Cokkinos DD, Antypa EG, Skilakaki M, et al. (2013) Contrast enhanced ultrasound of the kidneys: what is it capable of? Biomed Res Int 2013:595873
6. Brannigan M, Burns PN, Wilson SR (2004) Blood flow patterns in focal liver lesions at microbubble-enhanced US. Radiographics 24(4):921–935
7. Cosgrove D, Blomley M (2004) Liver tumors: evaluation with contrast-enhanced ultrasound. Abdom Imaging 29(4):446–454
8. Claudon M, Dietrich CF, Choi BI, et al. (2013) Guidelines and good clinical practice recommendations for Contrast Enhanced Ultrasound (CEUS) in the liver—update 2012: A WFUMB-EFSUMB initiative in cooperation with representatives of AFSUMB, AIUM, ASUM, FLAUS and ICUS. Ultrasound Med Biol 39(2):187–210
9. Wilson SR, Burns PN (2010) Microbubble-enhanced US in body imaging: what role? Radiology 257(1):24–39
10. Wei K, Mulvagh SL, Carson L, et al. (2008) The safety of deFinity and Optison for ultrasound image enhancement: a retrospective analysis of 78,383 administered contrast doses. J Am Soc Echocardiogr 21(11):1202–1206
11. U.S.National Institutes of Health (2014) SonoVue®-enhanced ultrasound versus unenhanced US for focal liver lesion characterization. https://clinicaltrials.gov/ct2/show/NCT00788697. Accessed 28 Dec 2014
12. U.S. Food and Drug Administration (2014) FDA approves a new ultrasound imaging agent (2014) http://www.fda.gov/NewsEvents/Newsroom/PressAnnouncements/ucm418509.htm. Accessed 28 Dec 2014. U.S. F.D.A. Lumason approval press release dated October 10, 2014
13. Claudon M, Cosgrove D, Albrecht T, et al. (2008) Guidelines and good clinical practice recommendations for contrast enhanced ultrasound (CEUS)—update 2008. Ultraschall Med 29(1):28–44
14. Bosniak MA (1986) The current radiological approach to renal cysts. Radiology 158(1):1–10
15. Bosniak MA (1993) Problems in the radiologic diagnosis of renal parenchymal tumors. Urol Clin North Am 20(2):217–230
16. Gabr AH, Gdor Y, Roberts WW, Wolf JS (2009) Radiographic surveillance of minimally and moderately complex renal cysts. BJU Int 103(8):1116–1119
17. Israel GM, Bosniak MA (2003) Follow-up CT of moderately complex cystic lesions of the kidney (Bosniak category IIF). Am J Roentgenol 181(3):627–633
18. Hartman DS, Choyke PL, Hartman MS (2004) From the RSNA refresher courses: a practical approach to the cystic renal mass. Radiographics 24(Suppl 1):S101–S115
19. Israel GM, Hindman N, Bosniak MA (2004) Evaluation of cystic renal masses: comparison of CT and MR imaging by using the Bosniak classification system. Radiology 231(2):365–371
20. Robbin ML, Lockhart ME, Barr RG (2003) Renal imaging with ultrasound contrast: current status. Radiol Clin North Am 41(5):963–978
21. Park BK, Kim B, Kim SH, et al. (2007) Assessment of cystic renal masses based on Bosniak classification: comparison of CT and contrast-enhanced US. Eur J Radiol 61(2):310–314
22. Quaia E, Bertolotto M, Cioffi V, et al. (2008) Comparison of contrast-enhanced sonography with unenhanced sonography and contrast-enhanced CT in the diagnosis of malignancy in complex cystic renal masses. Am J Roentgenol 191(4):1239–1249
23. Israel GM, Bosniak MA (2005) How I do it: evaluating renal masses. Radiology 236(2):441–450
24. Nicolau C, Bunesch L, Sebastia C (2011) Renal complex cysts in adults: contrast-enhanced ultrasound. Abdom Imaging 36(6):742–752
25. Clevert DA, Minaifar N, Weckbach S, et al. (2008) Multislice computed tomography versus contrast-enhanced ultrasound in evaluation of complex cystic renal masses using the Bosniak classification system. Clin Hemorheol Microcirc 39(1–4):171–178
26. Cairns P (2010) Renal cell carcinoma. Cancer Biomark 9(1–6):461–473
27. Russo P (2008) Contemporary understanding and management of renal cortical tumors. Urol Clin North Am 35(4):xiii–xvii
28. Ignee A, Straub B, Schuessler G, Dietrich CF (2010) Contrast enhanced ultrasound of renal masses. World J Radiol 2(1):15–31
29. Reese JH (1992) Renal cell carcinoma. Curr Opin Oncol 4(3):427–434
30. Ascenti G, Zimbaro G, Mazziotti S, et al. (2001) Usefulness of power Doppler and contrast-enhanced sonography in the differentiation of hyperechoic renal masses. Abdom Imaging 26(6):654–660
31. Forman HP, Middleton WD, Melson GL, McClennan BL (1993) Hyperechoic renal cell carcinomas: increase in detection at US. Radiology 188(2):431–434
32. Jinzaki M, Tanimoto A, Narimatsu Y, et al. (1997) Angiomyolipoma: imaging findings in lesions with minimal fat. Radiology 205(2):497–502
33. Xu ZF, Xu HX, Xie XY, et al. (2010) Renal cell carcinoma: real-time contrast-enhanced ultrasound findings. Abdom Imaging 35(6):750–756
34. Haendl T, Strobel D, Legal W, et al. (2009) Renal cell cancer does not show a typical perfusion pattern in contrast-enhanced ultrasound. Ultraschall Med 30(1):58–63
35. Fan L, Lianfang D, Jinfang X, Yijin S, Ying W (2008) Diagnostic efficacy of contrast-enhanced ultrasonography in solid renal parenchymal lesions with maximum diameters of 5 cm. J Ultrasound Med 27(6):875–885
36. Quaia E, Siracusano S, Bertolotto M, Monduzzi M, Mucelli RP (2003) Characterization of renal tumours with pulse inversion harmonic imaging by intermittent high mechanical index technique: initial results. Eur Radiol 13(6):1402–1412
37. Xu ZF, Xu HX, Xie XY, et al. (2010) Renal cell carcinoma and renal angiomyolipoma: differential diagnosis with real-time contrast-enhanced ultrasonography. J Ultrasound Med 29(5):709–717

38. Jiang J, Chen Y, Zhou Y, Zhang H (2010) Clear cell renal cell carcinoma: contrast-enhanced ultrasound features relation to tumor size. Eur J Radiol 73(1):162–167

39. Wang C, Yu C, Yang F, Yang G (2014) Diagnostic accuracy of contrast-enhanced ultrasound for renal cell carcinoma: a meta-analysis. Tumour Biol 35(7):6343–6350

40. Breda A, Treat EG, Haft-Candell L, et al. (2010) Comparison of accuracy of 14-, 18- and 20-G needles in ex-vivo renal mass biopsy: a prospective, blinded study. BJU Int 105(7):940–945

41. Choudhary S, Rajesh A, Mayer NJ, Mulcahy KA, Haroon A (2009) Renal oncocytoma: CT features cannot reliably distinguish oncocytoma from other renal neoplasms. Clin Radiol 64(5): 517–522

42. Tamai H, Takiguchi Y, Oka M, et al. (2005) Contrast-enhanced ultrasonography in the diagnosis of solid renal tumors. J Ultrasound Med 24(12):1635–1640

43. Wu Y, Du L, Li F, et al. (2013) Renal oncocytoma: contrast-enhanced sonographic features. J Ultrasound Med 32(3):441–448

44. Leekam RN, Matzinger MA, Brunelle M, Gray RR, Grosman H (1983) The sonography of renal columnar hypertrophy. J Clin Ultrasound 11(9):491–494

45. Ascenti G, Zimbaro G, Mazziotti S, et al. (2001) Contrast-enhanced power Doppler US in the diagnosis of renal pseudotumors. Eur Radiol 11(12):2496–2499

46. Jinzaki M, Ohkuma K, Tanimoto A, et al. (1998) Small solid renal lesions: usefulness of power Doppler US. Radiology 209(2): 543–550

47. Paspulati RM, Bhatt S (2006) Sonography in benign and malignant renal masses. Radiol Clin North Am 44(6):787–803

48. Simpson EL, Mintz MC, Pollack HM, Arger PH, Coleman BG (1986) Computed tomography in the diagnosis of renal pseudotumors. J Comput Tomogr 10(4):341–348

49. Tello R, Davison BD, O'Malley M, et al. (2000) MR imaging of renal masses interpreted on CT to be suspicious. Am J Roentgenol 174(4):1017–1022

50. Mazziotti S, Zimbaro F, Pandolfo A, et al. (2010) Usefulness of contrast-enhanced ultrasonography in the diagnosis of renal pseudotumors. Abdom Imaging 35(2):241–245

51. Barr RG, Peterson C, Hindi A (2014) Evaluation of indeterminate renal masses with contrast-enhanced US: a diagnostic performance study. Radiology 271(1):133–142

52. Bhatt S, MacLennan G, Dogra V (2007) Renal pseudotumors. Am J Roentgenol 188(5):1380–1387

53. Fontanilla T, Minaya J, Cortés C, et al. (2012) Acute complicated pyelonephritis: contrast-enhanced ultrasound. Abdom Imaging 37(4):639–646

54. Chassagne P, Perol MB, Doucet J, et al. (1994) Renal metastases from cancer. Apropos of 9 cases and review of the literature. Ann Med Interne 145(2):103–106

55. Morichetti D, Mazzucchelli R, Lopez-Beltran A, et al. (2009) Secondary neoplasms of the urinary system and male genital organs. BJU Int 104(6):770–776

56. Honda H, Coffman CE, Berbaum KS, Barloon TJ, Masuda K (1992) CT analysis of metastatic neoplasms of the kidney. Comparison with primary renal cell carcinoma. Acta Radiol 33(1):39–44

57. Wink MH, Laguna MP, Lagerveld BW, de la Rosette JJ, Wijkstra H (2007) Contrast-enhanced ultrasonography in the follow-up of cryoablation of renal tumours: a feasibility study. BJU Int 99(6):1371–1375

58. Barwari K, Wijkstra H, van Delden OM, de la Rosette JJ, Laguna MP (2013) Contrast-enhanced ultrasound for the evaluation of the cryolesion after laparoscopic renal cryoablation: an initial report. J Endourol 27(4):402–407

59. Chen Y, Huang J, Xia L, et al. (2013) Monitoring laparoscopic radiofrequency renal lesions in real time using contrast-enhanced ultrasonography: an open-label, randomized, comparative pilot trial. J Endourol 27(6):697–704

60. Dong XQ, Shen Y, Xu LW, et al. (2009) Contrast-enhanced ultrasound for detection and diagnosis of renal clear cell carcinoma. Chin Med J 122(10):1179–1183

61. Siracusano S, Bertolotto M, Ciciliato S, et al. (2011) The current role of contrast-enhanced ultrasound (CEUS) imaging in the evaluation of renal pathology. World J Urol 29(5):633–638

62. Cai Y, Du L, Li F, Gu J, Bai M (2014) Quantification of enhancement of renal parenchymal masses with contrast-enhanced ultrasound. Ultrasound Med Biol 40(7):1387–1393